

FULL PAPER

Quantitative Measure for Nonlinear Unstable Systems Based on the Region of Attraction and Its Application to Designing Parameter Optimization - Inverted Pendulum ExampleT. Horibe^a, B. Zhou^b, S. Hara^{a*} and D. Tsubakino^a^a*Department of Aerospace Engineering, Graduate School of Engineering, Nagoya University, Furo-cho, Chikusa-ku, Nagoya, 464-8603, Japan;* ^b*Department of Mechanical and Aerospace Engineering, University of California Los Angeles, Los Angeles, CA 90095, USA**(v1.0 released January 2013)*

Quantitative stability measures for mechanical systems are highly needed. However, only a few such measures have been proposed for nonlinear systems. In this paper, a quantitative measure of stability for nonlinear systems based on the region of attraction (ROA) is proposed, and the measure is applied to parameter optimization of mechanical systems: multi-link inverted pendulum example. Recently, some techniques for calculating ROAs have been suggested; however, obtaining an accurate estimate of a ROA remains computationally demanding. We illustrate two techniques for efficiently estimating the proposed measure and apply them to the design parameter optimization problem for maximizing the stability measure. A number of simulations show the effectiveness of the proposed method.

Keywords: design optimization; nonlinear systems; region of attraction; pendubot; multi-link inverted pendulum

1. Introduction

When designing any system, the inherent performance of the system should be considered. Thus, many researchers in the field of control theory have addressed the quantification of controllability. As is well known, the rank of the controllability matrix indicates whether the system is controllable or uncontrollable, but yields no further information. The concept of the degree of controllability was proposed to address this issue [1]; this measure is a quantitative index determining how easily a certain system can be controlled. Various definitions have been proposed for the degree of controllability measure; for example, there are definitions based on the energy required to control the system [2–5] or those based on the robustness against disturbances [6, 7]. These measures are accounted for when designing optimal structures, such as in the problem of an optimal arrangement of sensors and actuators for optimal control [8, 9].

The measures described above have been developed for linear systems and proved successful when designing several representative forms of mechanical structures. However, novel mechanical systems, likely with nontrivial characteristics, are expected in the future. A wheeled, inverted pendulum mobile robot [10, 11] or VTOL aircraft [12, 13] have been studied as examples of such novel mechanical systems. As these systems are inherently unstable and nonlinear, they should be stabilized by control for practical use. In these cases, the key point for the optimal design is the existence of a practical quantitative stability measure to treat nonlinear unstable systems. However, there have been only a few studies addressing this issue. Developing such quantitative

*Corresponding author. Email: haras@nuae.nagoya-u.ac.jp

stability measures is indispensable for introducing novel mechanical systems. In this paper, we take a first step toward this goal.

As a simple example, consider the problem of stabilizing a double inverted pendulum. This system consists of two pendulums arranged in series, and the stabilization problem in the upright position (unstable equilibrium) is often used as a benchmark control problem. The question that arises is about the combination of the lengths of the two pendulums that can be most easily controlled. One of the most important things in controlling a nonlinear unstable system is robustness against the nonlinearity of the system. In the regulation problem of such nonlinear unstable systems, there is no general design method for a globally stable control law that completely takes into account the nonlinearity of systems; linear control methods are often used around the equilibrium point of the system. In such a case, nonlinearity may jeopardize the stability of the system. Once the system is away from its linear response region, it is difficult to guarantee stability.

The region of attraction (ROA) is defined as a set of initial conditions for which a system is stable around a corresponding equilibrium point, and it occurs when a nonlinear, unstable system is controlled by a linear regulator. The size of the ROA indicates the robustness of the system with respect to the perturbation of initial conditions, with larger ROAs characterizing more easily stabilizable systems. Therefore, in this paper, focus on the ROA for stabilizing nonlinear systems and propose an ROA-based quantitative measure for stabilization. In general, however, the ROA has a complicated shape, which precludes its accurate estimation. Hence, we define *the minimal radius of the ROA* as the minimal length between the origin and the boundary of the ROA and consider this quantity as a measure of stability.

The existing methods for calculating ROAs fall into two categories: 1) numerical methods based on the Monte Carlo technique [14] and 2) analytical methods based on the Lyapunov approach [15–20]. Both of these methods have been used for characterizing a variety of systems [21, 22]. For the numerical methods, the Monte Carlo technique is one of the most popular methods; however, there is a tradeoff between the computation cost and the computation accuracy. The Lyapunov approach has been recently extended to polynomial systems [23–27] as these systems can be solved in the framework of linear matrix inequality (LMI) by using the sum of squares technique [28]. However, when handling high-dimensional systems, the dimension of matrix in semidefinite programming (SDP) become very large; hence, the computation is inherently difficult and often time-consuming. Although both of the above methods can be used to accurately calculate the shape of the ROA, they are not efficient when dealing with high-dimensional systems, owing to the increasing computation cost.

To address the above issues, this paper describes two types of estimation methods based on the minimal radius of the ROA. The first method is based on numerical calculations using Monte Carlo simulations and the bisection method. In this method, the computation cost is lowered by focusing not on finding the n -dimensional shape of the ROA but rather its minimal radius, which is defined by a one-dimensional parameter. The second method is based on the linear robustness analysis. This method can only be applied to polynomial systems up to the third order, thus, a polynomial approximation is needed to apply to non-polynomial systems. Furthermore, the estimated value is too conservative for use as an actual estimate of the minimal radius. However, the calculated value reflects the size of the minimal radius, and the value can be obtained from a simple algebraic calculation; thus, the cost of this computation is very low.

Our objective is to optimize the system design parameters for maximizing the minimal radius of the ROA. For the above double inverted pendulum problem, this amounts to finding the best length of the link that would yield the easiest stabilization. We estimated the minimal radius using the two methods described above and reported the optimization results for a multi-link inverted pendulum, a pendubot, and a quintuple inverted pendulum. Finally, we discuss the advantages and disadvantages of both methods in the context of optimization.

In Section 2, we explain the concepts of the ROA and its minimal radius, which we use as a quantitative measure of robustness. In Section 3, we demonstrate the two methods for calculating

the minimal radius: 1) the numerical approach based on the Monte Carlo technique and 2) the analytical approach based on the Lyapunov function. In Section 4, the measures calculated using the proposed methods are used for optimizing the design parameters of the system, maximizing the minimal radius of the ROA; the results of this optimization are reported for the pendubot and quintuple inverted pendulum on a hinge. We show that the proposed methods can efficiently optimize the system in terms of the minimal radius. For both of the proposed methods, we also discuss the trade-offs between the cost of computation and the computation accuracy.

2. The Region of Attraction and Its Minimal Radius

In this section, we describe a ROA-based quantitative measure for quantifying the robustness of a nonlinear system. The measure can be used as a reasonable index of robustness.

First, we introduce the concept of the ROA of a system. Consider the following autonomous nonlinear system:

$$\dot{x}(t) = f(x(t)), \quad x(0) = x_0 \quad \text{where } x \in \mathbb{R}^n, \quad f(\cdot) : \mathbb{R}^n \rightarrow \mathbb{R}^n. \quad (1)$$

Suppose $x = 0$ to be an asymptotically stable equilibrium point. Then, the ROA of the system is defined as

$$\Omega = \{x_0 \in \mathbb{R}^n \mid \lim_{t \rightarrow \infty} x(t) \rightarrow 0, \quad \dot{x} = f(x), \quad x(0) = x_0\}. \quad (2)$$

This definition says that if the initial condition of the system is in the ROA, i.e., $x_0 \in \Omega$, the states of the system asymptotically converge to the origin. ROAs exist in many nonlinear systems, such as the van der Pol system in the field of chaos or inverted pendulums in mechanical systems [29, 30]. Note that, in literature, this region is usually called the domain of attraction or the basin of attraction for the attractors. Many techniques for estimating ROAs have been suggested that allow estimating their shapes. Examples of these techniques are the Monte Carlo or sum of squares-based techniques. However, determining the exact shape of a ROA remains difficult.

In this paper, we do not deal with exact shapes but confine our interest to determining the narrowest dimension (worst-case stability), namely the minimal distance between the origin and the boundary of a ROA, as exemplified in Figure 1. We define the length as a *minimal radius* of the ROA and represent it by R_{\min} , that is

$$R_{\min} = \sup_{D(R) \in \Omega} R, \quad D(R) = \{x \in \mathbb{R}^n \mid \|x\| = R\} \quad (3)$$

where $\|\cdot\|$ is the Euclidean norm. We use the minimal radius as an index of the robustness of the system against nonlinear perturbations and seek to maximize it for design optimization. Smaller minimal radii reduce the ability to stabilize a system to only a small perturbation around the point of initial conditions. Note that other measures can also be considered, such as the ROA volume. However, consider the case of an extremely thin ROA with an infinite volume; systems that satisfy these conditions are practically unstable. In the following section, we describe the methods for estimating the minimal radius of the ROA.

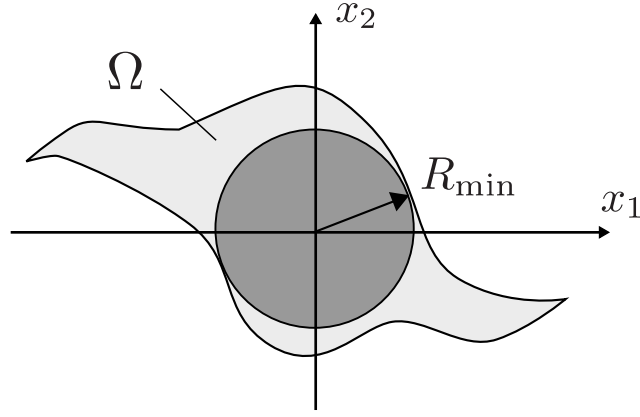


Figure 1. Region of attraction and its minimum radius

3. Methods for Estimating the Minimal Radius of the ROA

3.1 Monte Carlo Technique

As argued in introduction, when using the Monte Carlo method to accurately estimate the shape of the ROA, the calculation cost increases exponentially with the number of dimensions. Therefore, here we focus only on the minimal radius of the ROA and combine the Monte Carlo method with the bisection method to simplify the calculation. The rationale is that as the minimal radius depends only on a one-dimensional parameter, the calculation cost remains low even if the estimation accuracy is high.

Consider a region ∂D on a sphere with the radius R .

$$\partial D(R) = \{x_0 \in \mathbb{R}^n \mid \|x_0\| = R\} \quad (4)$$

Let R_{\min} be the minimal radius of the ROA. Then, $\partial D(R_{\min}) \subset \Omega$. Therefore, by updating the radius R of $\partial D(R)$ with the bisection method from an initial estimate, we can find the maximal R that satisfies $\partial D(R) \subset \Omega$. Then, R can be taken as an estimate of R_{\min} .

Figure 2 shows the flowchart for the method of estimating the minimal radius, and the method is explained below. The number of initial conditions for the Monte Carlo simulation and the number of iteration for the bisection method are denoted by N_{MC} and N_{BS} , respectively. First, define \bar{R}_{\min} and \bar{R}_{\max} as radii that are in and out of the ROA, respectively. Let $R_{\text{cur}} = (\bar{R}_{\min} + \bar{R}_{\max})/2$. Then, perform a simulation on the N_{MC} initial values $x_0 \in \partial D(R_{\text{cur}})$ and determine whether or not each point is included in the ROA. If divergence occurs even for one initial point, consider that $\partial D(R_{\text{cur}}) \not\subset \Omega$ and update \bar{R}_{\max} to R_{cur} . When convergence is observed for all n points, update \bar{R}_{\min} to R_{cur} . After updating, perform the Monte Carlo simulation again with $R_{\text{cur}} = (\bar{R}_{\min} + \bar{R}_{\max})/2$. Consequently, the value of the final \bar{R}_{\min} after N_{BS} iterations yields an estimate of the minimal radius, i.e., let $\bar{R}_{\min}^{k_i}$ be the k_i th minimum estimate in the bisection iteration, and let \hat{R}_{\min}^{MC} be the estimate of the Monte Carlo method; then

$$\hat{R}_{\min}^{MC} = \bar{R}_{\min}^{k_{N_{BS}}}. \quad (5)$$

The resolution of the bisection method can be obtained as $(R_{\max} - R_{\min})/2^{N_{BS}}$. We should also briefly mention how to decide the number of initial values when using the Monte Carlo method. The probability that the initial value exists inside the ROA follows the binomial distribution $B(N, p)$, where p is the probability that a single initial value exists inside the ROA, and N is the number of attempted initial values. Therefore, the probability that K initial values on ∂D

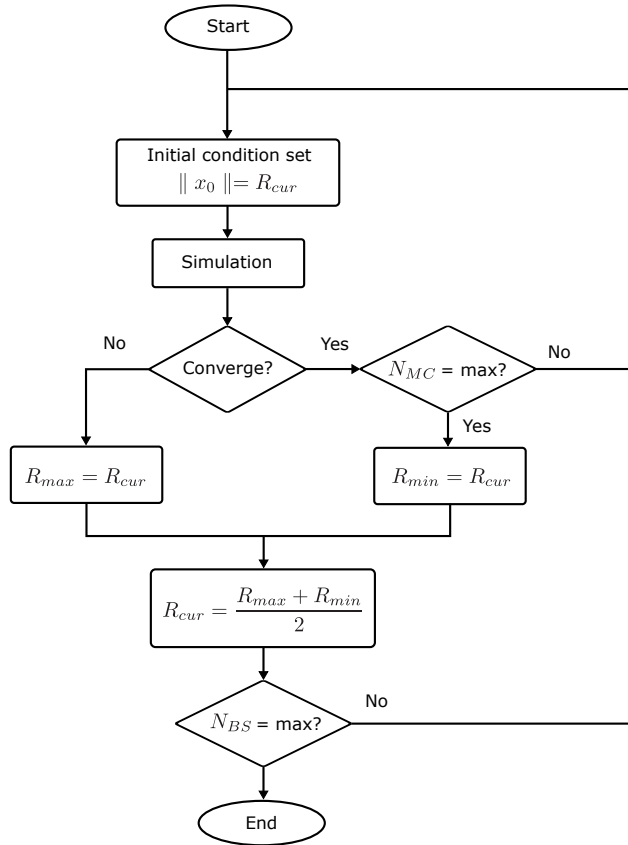


Figure 2. Programing flow of bisection method for estimating the minimum radius of the ROA

out of N are inside the ROA is given as

$${}_N C_K p^K (1-p)^{N-K}. \quad (6)$$

The probability that all of the N initial values converge ($K = N$) is p^N . Note that this probability p shows what percentage of ∂D is included in the ROA; thus, it can be said that *more than $p\%$ of ∂D is included in the ROA with $1 - p^N$ confidence*. According to this, for example, to say that 95% or more of D is included in the ROA with 99% confidence, the number of initial values should be $N \geq 90$.

It should be mentioned that estimating a ROA by an ellipse (not just a circle) is reasonable in some cases, which can be calculated by the Monte Carlo method by changing ∂D in (4) to an ellipse. It is, however, not clear how to define the parameter of the ellipse, and it may cause conservativeness when calculating the R_{\min} . Our goal is to compare the robustness of the nonlinear systems through the scalar value related to the ROA, which is R_{\min} in this paper. Thus, we directly estimate the R_{\min} by Monte Carlo without using the ellipse for the less conservativeness.

3.2 Linear Stability Analysis based on the Lyapunov Approach

Here, the minimal radius is approximately calculated by analyzing the stability of the system based on the Lyapunov approach. Some robustness measures have been proposed using the Lyapunov equation [31–33]. The following approach for estimating the ROA employs the Lyapunov-based stability analysis.

In this subsection, for analytical evaluation of the ROA, the application system class is limited to a polynomial system up to third order. We assume $f(x)$ in Eq.(1) is continuous and differ-

entiable, and the Jacobian linearization of the system around the equilibrium point $x = 0$ is asymptotically stable. The third-order approximated system then can be written as

$$\dot{x} = Ax + \tilde{f}(x), \quad (7)$$

where $A \in \mathbb{R}^{n \times n}$ is a linear coefficient matrix calculated as

$$A = \left. \frac{\partial f}{\partial x} \right|_{x=0}, \quad (8)$$

and $\tilde{f}(x)$ is a higher-order term, in which the i th column is written as

$$\tilde{f}_i(x) = \frac{1}{2!} \sum_{j,k} \left. \frac{\partial^2 f_i(x)}{\partial x_j \partial x_k} \right|_{x=0} x_j x_k + \frac{1}{3!} \sum_{j,k,l} \left. \frac{\partial^3 f_i(x)}{\partial x_j \partial x_k \partial x_l} \right|_{x=0} x_j x_k x_l. \quad (9)$$

Define the following Lyapunov function:

$$V(x) = x^T W x, \quad (10)$$

where $W \in \mathbb{R}^{n \times n}$, $W = W^T$ is the positive definite solution of the Lyapunov equation

$$A^T W + W A = -Q \quad (11)$$

with a positive definite matrix $Q \in \mathbb{R}^{n \times n}$. From equations (7) and (11), the time derivative of the Lyapunov function is

$$\dot{V}(x) = -x^T Q x + \tilde{f}(x)^T W x + x^T W \tilde{f}(x). \quad (12)$$

We rewrite $\tilde{f}(x)$ by using a state-dependent linear representation as

$$\tilde{f}(x) = E(x)x \quad (13)$$

so that the condition for the time derivative of the Lyapunov function to be negative is

$$x^T (E(x)^T W + W E(x)) x < x^T Q x. \quad (14)$$

To further examine the inequality (14), we prove the following lemma.

Lemma 1. *Let A and $\bar{A} \in \mathbb{R}^{n \times n}$ be symmetry matrices. Assume that the entries of \bar{A} are*

$$\bar{A}_{ij} \geq \begin{cases} A_{ij} & (i = j) \\ |A_{ij}| & (i \neq j). \end{cases} \quad (15)$$

Define a diagonal matrix B in which each diagonal entry B_{ii} is

$$B_{ii} = \sum_{j=1}^n \bar{A}_{ij}. \quad (16)$$

Then, for all $x \in \mathbb{R}^n$,

$$x^T A x \leq x^T B x. \quad (17)$$

Proof. Applying the Gershgorin Circle theorem to the matrix $B - A$ immediately gives the conclusion. \square

Use this lemma to examine (14). Define a symmetric matrix

$$H(x) = E(x)^T W + W E(x). \quad (18)$$

Since each (i, j) entry of $E(x)$ is composed of a linear and quadratic term of x , the entries of $H(x)$ (represented by $H_{ij}(x)$) can be written as a linear and quadratic term as well, i.e.,

$$H_{ij}(x) = h_{ij}^e{}^T x + x^T H_{ij}^e x \quad (19)$$

where $h_{ij}^e \in \mathbb{R}^n$ is a constant vector, and $H_{ij}^e \in \mathbb{R}^{n \times n}$ is a constant symmetric matrix. Let σ_{\max} and λ_{\max} be the maximal singular value and the eigenvalue, respectively. Define diagonal matrices $Z_1, Z_2 \in \mathbb{R}^{n \times n}$ so that each diagonal entry Z_{1ii} and Z_{2ii} is

$$Z_{1ii} = \sum_j \|h_{ij}^e\|, \quad (20)$$

$$Z_{2ii} = \lambda_{\max}(H_{ii}^e) + \sum_{i \neq j} \sigma_{\max}(H_{ij}^e). \quad (21)$$

Since

$$\|h_{ii}^e\| \|x\| + \lambda_{\max}(H_{ii}^e) \|x\|^2 \geq H_{ii}(x), \quad (22)$$

$$\|h_{ij}^e\| \|x\| + \sigma_{\max}(H_{ij}^e) \|x\|^2 \geq |H_{ij}(x)| \quad (23)$$

for all x , according to Lemma 1, we obtain

$$x^T H(x) x \leq x^T (Z_1 \|x\| + Z_2 \|x\|^2) x. \quad (24)$$

Consequently, from (14) and (24), a sufficient inequality condition for $\dot{V}(x) < 0$ is given as

$$x^T (Z_1 \|x\| + Z_2 \|x\|^2) x < x^T Q x. \quad (25)$$

Note that the above condition does not directly indicate ROA. That is, even if (25) is satisfied in the initial condition, the system may deviate from the region satisfying (25) in the transition process. Therefore, we consider the following elliptical region:

$$\Omega_W(\gamma) = \{x \in \mathbb{R}^n \mid x^T W x < \gamma\}. \quad (26)$$

We also introduce the following lemma to explain how to compute the ROA.

Lemma 2. ([34]) *Let the origin be a locally asymptotically stable equilibrium point of (1). Let*

$$\Omega_W(\gamma) \subseteq \{x \in \mathbb{R}^n \mid \dot{V}(x) < 0\} \cup \{0_n\}. \quad (27)$$

Then,

$$\Omega_W \subseteq \Omega. \quad (28)$$

Then, with the following theorem, $\Omega_W(\gamma)$ can serve as an estimate of the ROA.

Theorem 1. Consider an autonomous system described in (7). Define Q and W in (11), and Z_1, Z_2 in (20), (21) respectively. Assume that $f(x)$ is a third-order polynomial of x . Let $\gamma^* > 0$ be a scalar so that any $\gamma \in [0, \gamma^*]$ can satisfy the inequality

$$\gamma \lambda_{\max}(W^{-1}Z_2) + \sqrt{\gamma} \sqrt{\lambda_{\max}(W^{-1}Z_1)\lambda_{\max}(Z_1)} < \lambda_{\min}(Q). \quad (29)$$

Then, from any initial points $x_0 \in \Omega_W(\gamma^*)$, the system converges to the origin, i.e., $\Omega_W(\gamma^*)$ is an inner estimate of Ω .

Proof. Take a point x_b on the unit circle as $x_b \in \{x \in \mathbb{R}^n \mid \|x\| = 1\}$. Since $W > 0$, Ω_W is bounded, one point on the boundary of Ω_W can be written as αx_b with a positive scalar α . Then, α corresponding to x_b is given by

$$\alpha^2 x_b^T W x_b = \gamma. \quad (30)$$

The condition for satisfying (25) at the point $x = \alpha x_b$ is given as

$$\alpha^4 x_b^T Z_2 x_b + \alpha^3 x_b^T Z_1 x_b < \alpha^2 x_b^T Q x_b. \quad (31)$$

Therefore, by eliminating α from these two equations (30), (31), the condition for satisfying (25) with a given γ is obtained as

$$\gamma x_b^T Z_2 x_b + \sqrt{\gamma} x_b^T Z_1 x_b \sqrt{x_b^T W x_b} < x_b^T Q x_b x_b^T W x_b. \quad (32)$$

Since W is positive definite, this can be written as

$$\gamma \frac{x^T Z_2 x}{x^T W x} + \sqrt{\gamma} \sqrt{\frac{x^T Z_1 x}{x^T W x}} \sqrt{\frac{x^T Z_1 x}{x^T x}} < \frac{x^T Q x}{x^T x}. \quad (33)$$

Furthermore, W can be decomposed as $W = X^T X$ with a certain non-singular matrix $X \in \mathbb{R}^{n \times n}$. Let $y = Xx$. Note that $X^{-T} Z_i X^{-1}$ for $i = 1, 2$ is symmetric, then

$$\frac{x^T Z_i x}{x^T W x} = \frac{y^T X^{-T} Z_i X^{-1} y}{y^T y} \leq \lambda_{\max}(X^{-T} Z_i X^{-1}) = \lambda_{\max}\{X^{-1}(X^{-T} Z_i X^{-1})X\} = \lambda_{\max}(W^{-1} Z_i) \quad (34)$$

Therefore, since $\gamma > 0$, the sufficient condition of the inequality (33) is given as

$$\gamma \lambda_{\max}(W^{-1}Z_2) + \sqrt{\gamma} \sqrt{\lambda_{\max}(W^{-1}Z_1)\lambda_{\max}(Z_1)} < \lambda_{\min}(Q). \quad (35)$$

Since $Q > 0$, there exists $\gamma^* \in (0, +\infty)$ such that $\gamma \in [0, \gamma^*]$ satisfies (35). Then $\dot{V}(x) < 0$ holds anywhere in $\Omega_W(\gamma^*)$, and thus we can say $\Omega_W(\gamma^*) \subseteq \Omega$ from Lemma 2. \square

The inequality (29) in the theorem 1 is a second order for $\sqrt{\gamma}$, thus the condition of γ satisfying the inequality can be calculated analytically. For example, for an inverted pendulum system, $Z_1 = 0$ and $Z_2 > 0$, thus the condition of γ^* is given as

$$\gamma^* < \frac{\lambda_{\min}(Q)}{\lambda_{\max}(W^{-1}Z_2)}. \quad (36)$$

Let $\bar{\gamma} = \sup \gamma^*$. Then, $\Omega_W(\bar{\gamma})$ can serve as a reasonable estimate of the ROA. Since the region of Ω_W is an ellipse, the minimal radius $\hat{R}_{\min}^{LF}(\Omega_W)$ is estimated as

$$\hat{R}_{\min}^{LF}(\Omega_W) = \sqrt{\frac{\bar{\gamma}}{\lambda_{\max}(W)}}. \quad (37)$$

Note that, in this approach, the ROA is approximately estimated by an n -dimensional ellipse Ω_W ; the volume $V(\Omega_W)$ can be calculated easily as

$$V(\Omega_W) = \frac{\pi^{n/2}}{\Gamma(n/2 + 1)} \sqrt{\det(W^{-1}\bar{\gamma})}, \quad (38)$$

and it can be a reasonable measure of the ROA in some cases.

4. Structure Optimization

4.1 Pendubot Example

In this section, design parameter optimization based on the minimal radius of the ROA is considered for mechanical system examples. As an example of low-dimensional nonlinear mechanical system, we consider a pendubot [35]. The schematic is shown in Figure 3. For the i -th link ($i = 1, 2$), q_i is the angle (define $q = [q_1, q_2]^T$), m_i is the mass, l_i is the length, l_{c_i} is the distance from the i -th joint to the center of mass (COM), J_i is the inertia around the center of mass, and g is the gravitational acceleration ($= 9.801 \text{ m/s}^2$). This system has two links connected in series and moves symmetrically in a plane. The control input (torque τ) is only on the joint connected to the inertial reference frame, and the joint between links rotates freely.

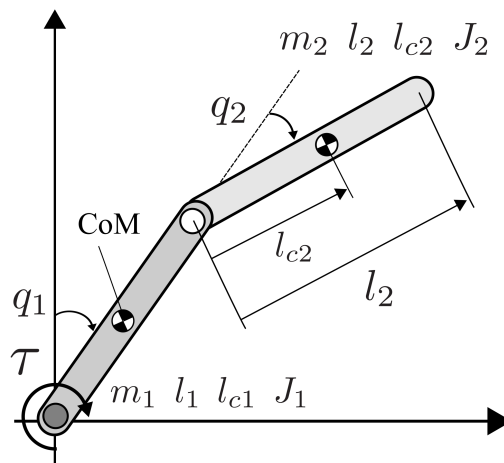


Figure 3. The schematic of the pendubot

A pendubot is a so-called underactuated system, and the problem of stabilizing at an unstable equilibrium point, where two links stand vertically, is often treated as a benchmark problem of nonlinear control. Some methods have been proposed for solving this stabilization problem for the pendubot [36–38]; however, a global stabilization principle that fully accounts for the nonlinearity of the system is not yet known, and stabilization by linear control is usually performed around the origin. In this case, the stability of the system strongly depends on the system parameters. Consider, for example, the case in which the first link (l_1) connected to the reference frame is very short and the second link (l_2) is very long. Then, for a small perturbation in the initial value

of the second link, the first link needs to move significantly to transmit the torque to the second link. This motion induces nonlinearity, and the region that can be stabilized by linear control is considered very small. Our objective is to investigate the best length relationship between the two links that will yield the easiest stabilization by linear control.

Using the method of Lagrange, the equation of motion of the pendubot is derived as follows:

$$M(q_2)\ddot{q} + C(q, \dot{q})\dot{q} + G(q) = u, \quad (39)$$

where $u = [\tau, 0]^T$ and

$$M(q_2) = \begin{bmatrix} M_{11}(q_2) & M_{12}(q_2) \\ M_{21}(q_2) & M_{22} \end{bmatrix} = \begin{bmatrix} a_1 + a_2 + 2a_3 \cos q_2 & a_2 + a_3 \cos q_2 \\ a_2 + a_3 \cos q_2 & a_2 \end{bmatrix}$$

$$C(q, \dot{q}) = \begin{bmatrix} -a_3\dot{q}_2 \sin q_2 + \mu_1 & -a_3(\dot{q}_1 + \dot{q}_2) \sin q_2 \\ a_3\dot{q}_1 \sin q_2 & \mu_2 \end{bmatrix}, \quad G(q) = \begin{bmatrix} -b_1 \sin q_1 - b_2 \sin(q_1 + q_2) \\ -b_2 \sin(q_1 + q_2) \end{bmatrix},$$

$$a_1 = m_1 l_{c1}^2 + m_2 l_1^2 + J_1, \quad a_2 = m_2 l_{c2}^2 + J_2,$$

$$a_3 = m_2 l_1 l_{c2}, \quad b_1 = (m_1 l_{c1} + m_2 l_1)g, \quad b_2 = m_2 l_{c2}g,$$

where μ_1 and μ_2 are the viscosity coefficients for the corresponding joints. Let $x = [x_1, x_2, x_3, x_4]^T = [q_1, q_2, \dot{q}_1, \dot{q}_2]^T$ be state variables. Then, the state space representation of this system is given as

$$\dot{x} = f(x) + g(x)\tau, \quad (40)$$

where

$$f(x) = \begin{bmatrix} x_3 \\ x_4 \\ -M(q_2)^{-1} [C(q, \dot{q})\dot{q} + G(q)] \end{bmatrix}, \quad g(x) = \begin{bmatrix} 0 \\ 0 \\ M(q_2)^{-1} \begin{bmatrix} 1 \\ 0 \end{bmatrix} \end{bmatrix}. \quad (41)$$

For optimizing the lengths of the links, we introduce some assumptions. Assume that each link is a cylinder with uniform density ρ and radius r ; thus, the mass is written as $m_i = \pi r^2 \rho l_i$, and $l_{ci} = l_i/2$, $J_i = m_i l_i^2/12$. Further, the viscous friction of the shaft on which the motor is mounted is considered to be large; therefore we set the viscosity coefficients for the joints as $\mu_1 = 0.2$ and $\mu_2 = 0.01$, respectively. In the following calculation, the physical parameters are $r = 4$ mm, and $\rho = 2.70$ g/cm³, and the closed loop is designed to be stable around the origin (inverted point) with the LQR controller minimizing the cost function $J = \int_0^\infty x^T Q_{lq} x + \tau^T R_{lq} \tau dt$. The weight matrix of the corresponding problem is

$$Q_{lq} = \begin{bmatrix} 1 & 0 & 0 & 0 \\ 0 & 1 & 0 & 0 \\ 0 & 0 & 1 & 0 \\ 0 & 0 & 0 & 1 \end{bmatrix}, \quad R_{lq} = 1. \quad (42)$$

Then, the closed loop system is written as

$$\dot{x} = f(x) - g(x)Kx, \quad (43)$$

where K is the feedback gain calculated by LQR method. We examine the ROA of this system. When use the Lyapunov based approach, the third-order Taylor approximation is applied to the system as described in section 3.2 .

First, we simulate the equation (43) for some initial conditions and visualize the ROA of the pendubot in a zero angular velocity slice, with link lengths $l_1 = l_2 = 1$ m. The ROA, obtained from numerical calculations at each initial point $x_0 = [q_1(0), q_2(0), 0, 0]$, is shown in Figure 4. The colored area indicates the point to which the system converges from the corresponding initial condition. We also show the minimal radius of the ROA estimated using the Monte Carlo method ($N_{MC} = 1000$, $N_{BC} = 12$), which is calculated as $\hat{R}_{\min}^{MC} = 0.53$.

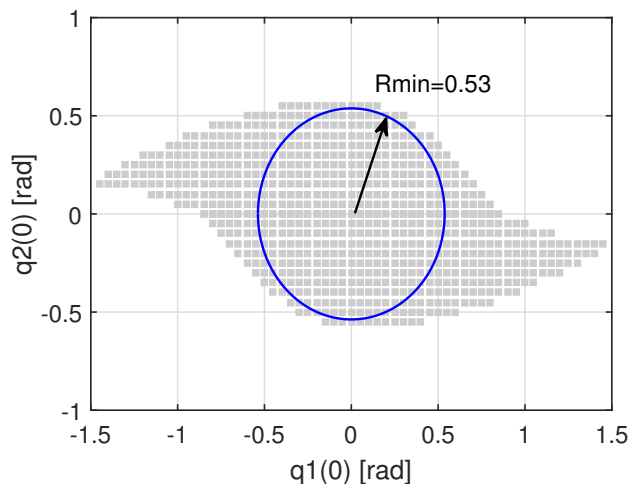


Figure 4. The ROA for the pendubot (zero angular velocity slice) with link lengths $l_1 = 1$ m, $l_2 = 1$ m, and LQR control in which the weight matrices are $Q = I_{4 \times 4}$ and $R = 1$

Next, we consider the link lengths l_1 and l_2 as optimization variables and find the ones that maximized R_{\min} in the admissible range. Here, the range is $l_1 \in [0.1, 1.0]$ and $l_2 \in [0.1, 1.0]$; the grid search method is used to determine the optimal link lengths. For each grid point, the proposed measures \hat{R}_{\min}^{MC} (5) and \hat{R}_{\min}^{LF} (37) are calculated for the system (43), and the results are shown in Figure 5. Note that the feedback gain K is calculated for each grid, corresponding to the optimization variables l_1 and l_2 .

In the Monte Carlo method computation, the parameters are $N_{MC} = 100$, and $N_{BS} = 10$.

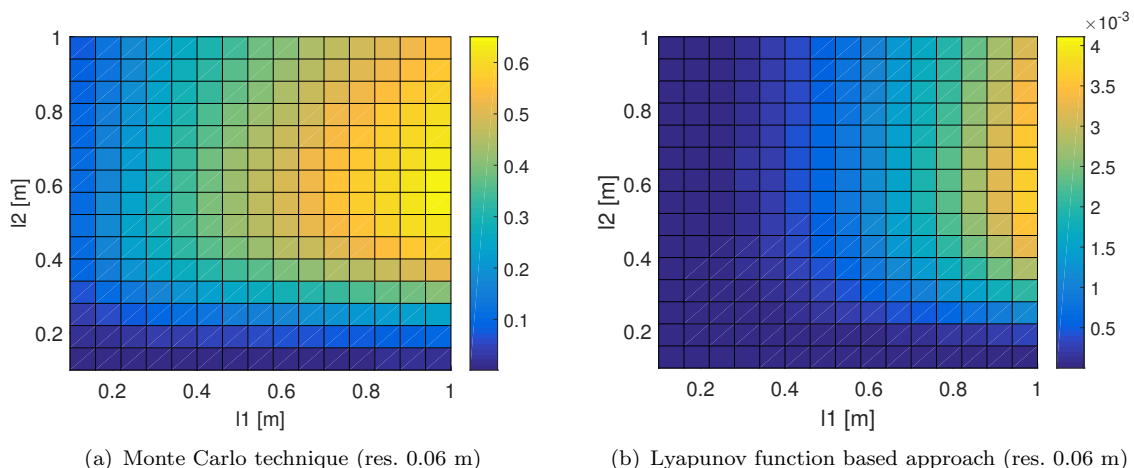


Figure 5. The grid search results for the estimation of the minimal radius using the (a) Monte Carlo technique \hat{R}_{\min}^{MC} and (b) Lyapunov function-based technique \hat{R}_{\min}^{LF} . The resolution in the grid search was 0.06 m in both calculations. The overall computation time is ~ 15 h for (a) and ~ 3.4 s for (b) using MATLAB.

The optimal value is computed as $\hat{R}_{\min}^{MC} = 0.64$ for $l_1 = 1.0$ and $l_2 = 0.58$. On the other hand, in the Lyapunov-based method computation, the Lyapunov equation (11) is solved with $Q = I_{4 \times 4}$. The nonlinear term $\tilde{f}(x)$ of the system (43) is approximated to be a cubic function by Taylor series expansion, and the optimal value is $\hat{R}_{\min}^{LF} = 4.1 \times 10^{-3}$ for $l_1 = 1.0$ and $l_2 = 0.52$. Note that the value obtained using the Lyapunov-based method is too small compared with one obtained using the Monte Carlo method for use as an actual estimate of the minimal radius. However, the tendency in the distribution of values for the Lyapunov-based method (Figure 5(b)) resembles the value calculated using the Monte Carlo method (Figure 5(a)) and thus can be used as a guide for finding the optimal link lengths. The computation time required for the Monte Carlo calculation is ~ 15 h. On the other hand, the time required for the Lyapunov-based method is ~ 3.4 s. These codes are written in Matlab R2016a and performed in a PC with Intel Core i7-6700 processor 3.40 GHz, 8 GB of RAM. It is seen that the computation cost of the Lyapunov-based method is very low compared to the one of the Monte Carlo method. Therefore, the Lyapunov-based method may be used as a rough estimate of the preliminary stage for accurately calculating the minimal radius using the Monte Carlo method for the optimization. The ROA with the optimized link lengths shown in Figure 6, confirming that R_{\min} is increased by the optimization.

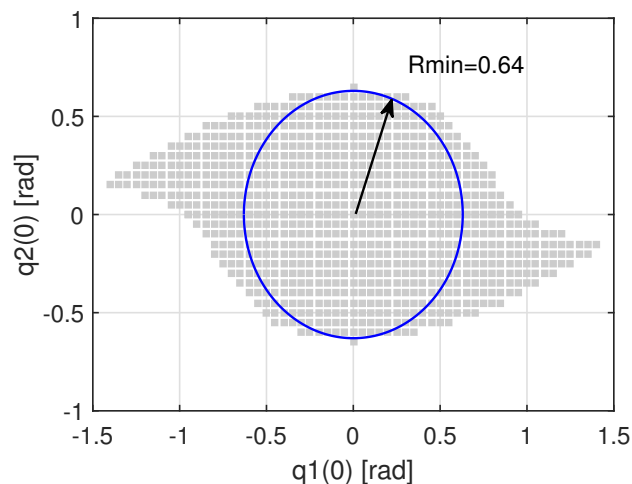


Figure 6. The ROA for the pendubot (zero angular velocity slice) with *optimised* link lengths $l_1 = 1$ m, $l_2 = 0.58$ m and LQR control in which the weight matrices $Q = I_{4 \times 4}$ and $R = 1$.

For further study of the optimal pendubot configuration, we calculated several cases with different viscous coefficients, and it is found μ_2 rather than μ_1 has a great influence on the optimal configuration and minimal radius. In addition, $l_1 = 1$ (upper limit) is given as an optimal value in most cases. Figure 7 shows the optimal second link length l_2 and R_{\min} for different viscous coefficients μ_2 calculated by both methods proposed in this paper (μ_1 is set to 0). It is shown Lyapunov function based approach follows the same tendency as the Monte Carlo method's result.

We give a physical interpretation for this result. In the ideal (no friction) case that $\mu_1 = \mu_2 = 0$, if l_1 is relatively long for the unactuated link l_2 , the movement of l_1 needed to stabilize l_2 is small and the motion is close to linear. Hence it is reasonable that the length of l_1 is the upper limit value and l_2 is small value. On the other hand, when a viscous friction exists on the angle between the links, if the length of l_2 is extremely small, the motion of l_1 can not be transmitted to the angle q_2 because of the friction. The optimum value is determined considering this trade-off well.

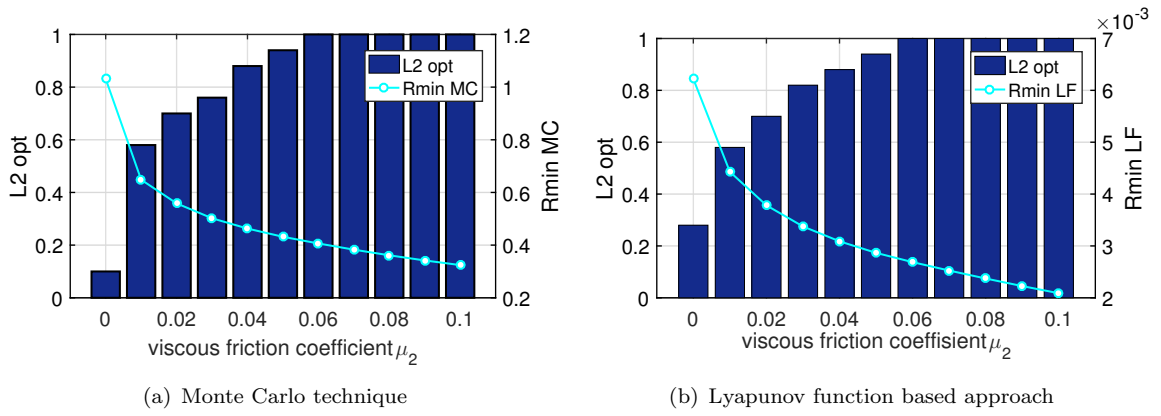


Figure 7. The optimal configuration of the pendubot for different viscous friction coefficients μ_2 calculated by (a) Monte Carlo technique and (b) Lyapunov function based approach. In both method, $\mu_1 = 0$ is set, and $l_1 = 1$ is given as optimal for all cases.

4.2 Optimization of the Quintuple Inverted Pendulum on a Hinge System using the Genetic Algorithm

Through the previous pendubot example, we confirmed that the two proposed measures could be used for the parameter optimization. Next, we apply these methods to the optimization of higher-dimensional systems, taking as an example a quintuple inverted pendulum. However, the grid search method can be no longer used here owing to its high computation cost. Thus, we use the genetic algorithm approach for the parameter optimization of this system. The schematic of the 5-link inverted pendulum is shown in Figure 8. The index of the link of the hinge is set to 0, and other links are numbered 1 to 5, starting from the bottom as in figure.

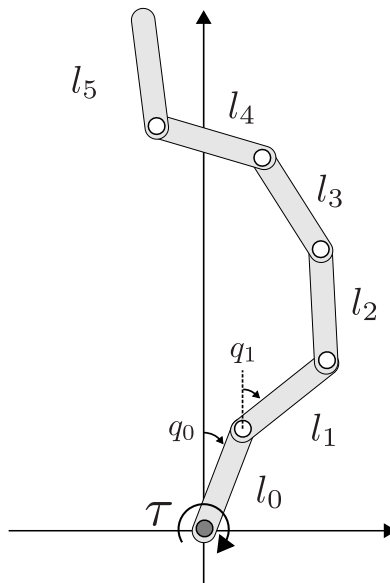


Figure 8. The schematic model of a quintuple inverted pendulum on a hinge. q_i ($i = 0 \sim 5$) is the deviation angles of the i -th links from the upright position.

The system is mounted on a hinge with five rotating links, which can be regarded as the extension of a pendubot to six links. For the general multi-link inverted pendulum system, the nonlinear dynamics is studied in [39–41], and the linear controllability and observability are studied in [42]. According to those study, this 6-link inverted pendulum configuration is linearly controllable and observable in the upward position. As a control achievement of a multi-link inverted pendulum, stabilization experiment of a quadruple inverted link on a cart was reported in [43]. The stabilization at the inverted position was achieved by fuzzy control in that paper.

Table 1. Parameter of Genetic Algorithm

Parameter	Value/Scheme
Population	200
Number of generations	15
Number of offspring	160
Selection scheme	Roulette wheel
Crossover scheme	Intermediate
Mutation	White Gaussian noise
Variance of mutation	0.01

However, there was no description of the proper design method for determining the links lengths. Here, as in the case of the pendubot, our objective is to find the optimal link lengths maximizing the minimal radius of the ROA, assuming that the closed loop is stabilized by the LQR controller with the identity weight matrix ($Q_{lq} = I_{12 \times 12}$, $R_{lq} = 1$).

The links are assumed to have uniform density, and other parameters such as inertia and mass are set in the same manner as in the pendubot case. The viscosity coefficients for the joints are $\mu_0 = 0.2$ and $\mu_i = 0.01$ ($i = 1, \dots, 5$). Thus, the design parameter are the lengths of the six links ($l_0 \sim l_5$). We also consider the motor kinematics mounted on a hinge. Denoting the gear ratio and the inertia of the motor by n and J_m , respectively, the apparent inertia J_0^a of the hinge is written as

$$J_0^a = J_0 + n^2 J_m, \quad (44)$$

where $J_0 (= m_0 l_0^2 / 12)$ is the original inertia of the hinge. We use this apparent value J_0^a as the inertia of the hinge with $n = 28$ and $J_m = 7.96 \times 10^{-6} \text{ kg} \cdot \text{m}^2$.

In the genetic algorithm calculation, linear constraint conditions for the length of each link length are set as follows:

$$0.1 \leq l_0, l_1, \dots, l_5 \leq 1.0, \quad \sum_{i=0}^5 l_i \leq 1.5 \quad (45)$$

Therefore, each link has to be longer than 0.1 m, and the total length has to be shorter than 1.5 m. For the crossover process of the GA, an intermediate method is used as

$$\text{child1} = \text{parent1} + \text{rand} * (\text{parent2} - \text{parent1}) \quad (46)$$

where rand is an uniform random number in the 0-1 range, having the children satisfy a supra-linear constraint. The mutation rate is set to 0.1, and Gaussian noise with a variance of 0.01 is added in the mutation process. For other details of the GA algorithm, see Table 1.

The parameters in the Monte Carlo method are $N_{MC} = 100$ and $N_{BC} = 10$, and the fitness value of the GA is defined by R_{\min}^{MC} (5) in this problem. The result of optimization performed using the Monte Carlo method and GA is shown in Figure 9. Figure 10 also shows the best fitness values of the optimal individuals, for each generation.

The results obtained using the Lyapunov-based method are shown in Figures 11 and 12. Here, the value of the fitness function is defined by R_{\min}^{LF} (37), and the positive definite matrix Q in the Lyapunov equation is chosen to be the identity matrix. Clearly, the optimal links lengths yielded by the two methods are similar, with the third link being the longest, ~ 0.6 m. The next longest is the hinge, ~ 0.4 m, and the other links are almost of the minimal allowable length, ~ 0.1 m. However, the calculation times are dramatically different, with the Monte Carlo method completing in more than 112 h, but Lyapunov-based method completing in 6.4 h.

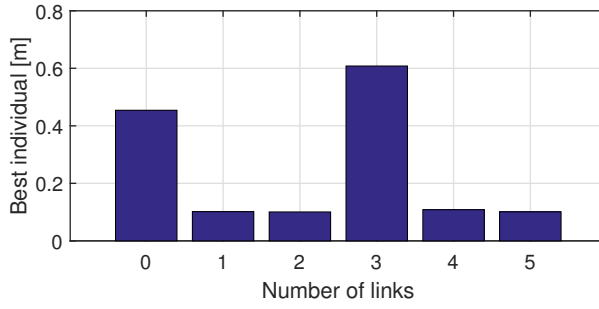


Figure 9. Results of the Monte Carlo calculation. Optimal link lengths: $l_0 = 0.4434$, $l_1 = 0.1018$, $l_2 = 0.1007$, $l_3 = 0.6162$, $l_4 = 0.1121$, $l_5 = 0.1012$

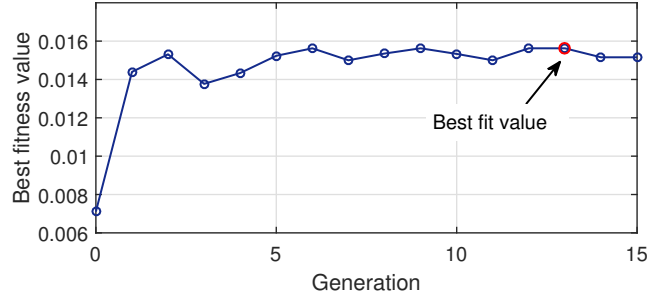


Figure 10. Results of the Monte Carlo calculation. Best individual value vs. the generation number. The best fitness value is 0.01563, the overall calculation time was 112.3 h

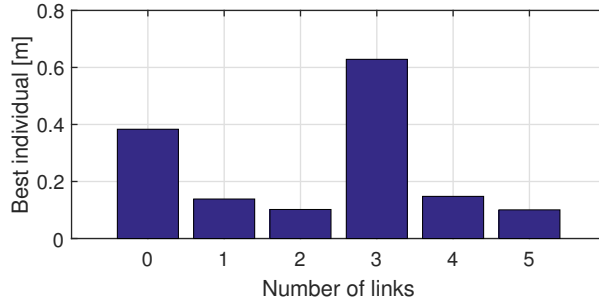


Figure 11. Results of the Lyapunov-based method. Optimal link lengths: $l_0 = 0.3833$, $l_1 = 0.1386$, $l_2 = 0.1019$, $l_3 = 0.6285$, $l_4 = 0.1479$, $l_5 = 0.1006$

To evaluate the results of these optimizations, the values of R_{\min} are calculated and compared for four cases: two optimized cases, and "equally divided" and "sweep" cases. The links lengths in the "equally divided" scenario are set to be the same, while in the "sweep" scenario the links gradually become longer, with the bottom link being the shortest.

The value of R_{\min} is calculated more accurately using the Monte Carlo method as \hat{R}_{\min}^{MC} with $N_{MC} = 1000$ and $N_{BC} = 12$. The results are summarized in Table 2. The largest \hat{R}_{\min}^{MC} is the one obtained using the Monte Carlo method, and the obtained value is $\hat{R}_{\min}^{MC} = 0.01313$. The value obtained using the Lyapunov-based method is also $\hat{R}_{\min}^{MC} = 0.01252$, considerably close to that obtained using the Monte Carlo method. In both case, the values of \hat{R}_{\min}^{MC} are four times larger than those obtained in the "equally divided" scenario, making the optimization evident.

Because the Monte Carlo method calculates the minimal radius of the ROA considering all nonlinearity, it can provide a very accurate estimation, but it is still impossible to prevent an increase in the computation time. On the other hand, because the method based on the Lyapunov function requires using a rough approximation, the estimated value is very conservative in the sense of the ROA approximation; however, it is still useful in terms of the computation cost for use as a guideline for optimization.

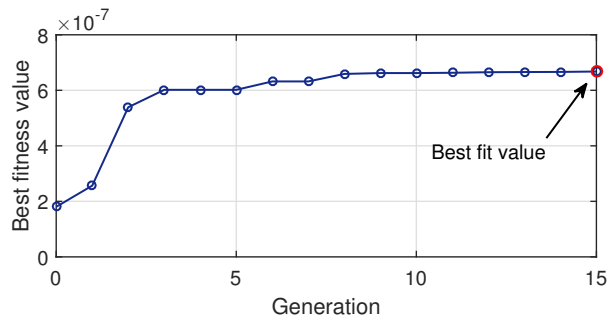


Figure 12. Results obtained using the Lyapunov-based method. Best individual value vs. the generation number. The best fitness value is 6.69×10^{-7} , and the overall calculation time is 6.4 h

Table 2. Link lengths and minimal radii of ROA

	l_0	l_1	l_2	l_3	l_4	l_5	\hat{R}_{\min}^{MC*}	Calc time**
Monte Carlo opt	0.4542	0.1017	0.1007	0.6080	0.1084	0.1009	0.01313	112.3 hour
Lyapunov opt	0.3831	0.1385	0.1018	0.6282	0.1478	0.1005	0.01252	6.4 hour
Equally divided	0.1500	0.1500	0.1500	0.1500	0.1500	0.1500	0.00314	-
Sweep	0.1000	0.1000	0.2500	0.2500	0.4000	0.4000	0.00289	-

* An accurate estimate was calculated using the Monte Carlo method with $N_{MC} = 1000$, $N_{BS} = 12$

** Computation was performed by parallel computing using 4 cores with Paralel Computing Toolbox of MATLAB

5. Conclusion

As a quantitative measure of the stability of nonlinear unstable systems, the minimal radius of the ROA was adopted here. Two types of approximate calculation methods for the minimal radius were considered, and calculations were performed for the pendubot and the quintuple inverted pendulum systems. Comparing those results, it was shown that both of the considered methods were able to calculate the optimal lengths of links in multiple inverted pendulum systems. However, the Monte Carlo method and the Lyapunov-based method have a trade-off between accuracy and computation cost, and more efficient optimization may be possible by successfully combining them.

Acknowledgement

The second author sincerely appreciates the Japan-US Advanced Collaborative Education Program (JUACEP) in Nagoya University and University of California Los Angeles for providing this opportunity to study this topic.

References

- [1] Viswanathan CN, Longman RW, Linkins PW. A degree of controllability definition: fundamental concepts and application to model systems. *Journal of Guidance, Control, and Dynamics*. 1984; 7(2):222–230.
- [2] Zhou K, Salomon G, Wu E. Balanced realization and model reduction for unstable systems. *International Journal of Robust and Nonlinear Control*. 1999;9(3):183–198.
- [3] Lee H, Park Y. Degree of controllability for linear unstable systems. *Journal of Vibration and Control*. 2016;22(7):1928–1934.
- [4] Chen J, Hara S, Chen G. Best tracking and regulation performance under control energy constraint. *IEEE Transactions on Automatic Control*. 2003;48(8):1320–1336.
- [5] Singh AK, Hahn J. Determining optimal sensor locations for state and parameter estimation for stable nonlinear systems. *Industrial and Engineering Chemistry Research*. 2005;44(15):5645–5659.

- [6] Kang O, Park Y, Park YS, Suh M. New measure representing degree of controllability for disturbance rejection. *Journal of Guidance, Control, and Dynamics*. 2009;32(5):1658–1661.
- [7] Bakhtiar T, Hara S. H_2 regulation performance limitations for SIMO linear time-invariant feedback control systems. *Automatica*. 2008;44(3):659–670.
- [8] Hac A, Liu L. Sensor and actuator location in motion control of flexible structures. *Journal of Sound and Vibration*. 1993;167(2):239–261.
- [9] van de Wal M, de Jager B. A review of methods for input/output selection. *Automatica*. 2001;37(4):487–510.
- [10] Pathak K, Franch J, Agrawal SK. Velocity and position control of a wheeled inverted pendulum by partial feedback linearization. *IEEE Transactions on Robotics*. 2005;21(3):505–513.
- [11] Grasser F, D’Arrigo A, Colombi S, Rufer A. JOE: A mobile, inverted pendulum. *IEEE Transactions on Industrial Electronics*. 2002;49(1):107–114.
- [12] Cetinsoy E, Dikyar S, Hancer C, Oner K, Sirimoglu E, Unel M, Aksit M. Design and construction of a novel quad tilt-wing UAV. *Mechatronics*. 2012;22(6):723–745.
- [13] Ailon A. Simple tracking controllers for autonomous VTOL aircraft with bounded inputs. *IEEE Transactions on Automatic Control*. 2010;55(5):737–743.
- [14] Armiyoon AR, Wu CQ. A novel method to identify boundaries of basins of attraction in a dynamical system using Lyapunov exponents and Monte Carlo techniques. *Nonlinear Dynamics*. 2015;79(1):275–293.
- [15] Zecevic AI, Siljak DD. Estimating the region of attraction for large-scale systems with uncertainties. *Automatica*. 2010;46(2):445–451.
- [16] Amato F, Cosentino C, Merola A. On the region of attraction of nonlinear quadratic systems. *Automatica*. 2007;43(12):2119–2123.
- [17] Vannelli A, Vidyasagar M. Maximal Lyapunov functions and domains of attraction for autonomous nonlinear systems. *Automatica*. 1985;21(1):69–80.
- [18] Davison EJ, Kurak EM. A computational method for determining quadratic Lyapunov functions for non-linear systems. *Automatica*. 1971;7(5):627–636.
- [19] Genesio R, Tartaglia M, Vicino A. On the estimation of asymptotic stability regions: State of the art and new proposals. *IEEE Transactions on Automatic Control*. 1985;30(8):747–755.
- [20] Topcu U, Packard AK, Seiler P, Balas GJ. Robust region-of-attraction estimation. *IEEE Transactions on Automatic Control*. 2010;55(1):137–142.
- [21] Shamaghdari S, Nikravesh SKY. A nonlinear stability analysis of elastic flight vehicle. *Aircraft Engineering and Aerospace Technology*. 2012;84(6):404–412.
- [22] Chakraborty A, Seiler P, Balas G. Nonlinear region of attraction analysis for flight control verification and validation. *Control Engineering Practice*. 2011;19(4):335–345.
- [23] Chesi G. Rational Lyapunov functions for estimating and controlling the robust domain of attraction. *Automatica*. 2013;49(4):1051–1057.
- [24] Chesi G. *Domain of attraction: Analysis and control via SOS programming*. Springer. 2011.
- [25] Hachicho O. A novel LMI-based optimization algorithm for the guaranteed estimation of the domain of attraction using rational Lyapunov functions. *Journal of the Franklin Institute*. 2007;344(5):535–552.
- [26] Tan W, Packard A. Stability region analysis using polynomial and composite polynomial lyapunov functions and sum-of-squares programming. *IEEE Transactions on Automatic Control*. 2008;53(2):565–571.
- [27] Topcu U, Packard A, Seiler P. Local stability analysis using simulations and sum-of-squares programming. *Automatica*. 2008;44(10):2669–2675.
- [28] Parrilo PA. Semidefinite programming relaxations for semialgebraic problems. *Mathematical Programming*. 2003;96(2):293–320.
- [29] Chesi G. Estimating the domain of attraction for non-polynomial systems via LMI optimizations. *Automatica*. 2009;45(6):1536–1541.
- [30] Khodadadi L, Samadi B, Khaloozadeh H. Estimation of region of attraction for polynomial nonlinear systems: a numerical method. *ISA Transactions*. 2014;53(1):25–32.
- [31] Patel RV, Toda M. Quantitative measures of robustness for multivariate systems. In: *Proc. joint automatic control conference*. San Francisco, CA. 1980. TP8-A.
- [32] Bernstein DS, Haddad WM. Robust stability and performance analysis for linear dynamic systems. *IEEE Transactions on Automatic Control*. 1989;34(7):751–758.
- [33] Gajic Z, Qureshi MTJ. *Lyapunov matrix equation in system stability and control*. Academic Press.

- 1995.
- [34] Khalil HK. Nonlinear systems. Prentice Hall. 2001.
 - [35] Spong MW, Block DJ. The pendubot: A mechatronic system for control research and education. In: Proc. IEEE Conference on Decision and Control . 1995. p. 555–557.
 - [36] Zhang M, Tarn TJ. Hybrid control of the pendubot. IEEE/ASME Transactions on Mechatronics. 2002;7(1):79–86.
 - [37] Fantoni I, Lozano R, Spong MW. Energy based control of the pendubot. IEEE Transactions on Automatic Control. 2000;45(4):725–729.
 - [38] Albahkali T, Mukherjee R, Das T. Swing-up control of the pendubot: An impulse momentum approach. IEEE Transactions on Robotics. 2009;25(4):975–982.
 - [39] Eltohamy KG, Kuo CY. Nonlinear generalized equations of motion for multi-link inverted pendulum systems. International Journal of Systems Science. 1999;30(5):505–513.
 - [40] Larcombe PJ. On the control of a two dimensional multi-link inverted pendulum: co-ordinate system suitability for dynamic formulation. International Journal of Systems Science. 1992;23(12):2265–2289.
 - [41] Lam S, Davison EJ. The real stabilizability radius of the multi-link inverted pendulum. In: Proc. of the 2006 American Control Conference. Minneapolis, Minnesota, USA. 2006 June 14-16. WeC12.3.
 - [42] Liu Y, Xin X. Controllability and observability of an n-link planar robot with a single actuator having different actuatorsensor configurations. IEEE Transactions on Automatic Control. 2016;61(4):1129–1134.
 - [43] Zhang Y, Wang J, Li H. Stabilization of the quadruple inverted pendulum by variable universe adaptive fuzzy controller based on variable gain H_∞ regulator. Journal of Systems Science and Complexity. 2012;25(5):856–872.